

Functionalized 4-(Dialkylamino)-4'-nitrostilbenes as Reactive Fluorescent Probes for Monitoring the Photoinitiated Polymerization of MMA

Wolter F. Jager*

Department of Polymer Technology, Delft University of Technology, Julianalaan 136, 2628 BL Delft, The Netherlands

Ananda M. Sarker and Douglas C. Neckers*

Center for Photochemical Sciences, Bowling Green State University, Bowling Green, Ohio 43403

Received May 17, 1999; Revised Manuscript Received October 6, 1999

ABSTRACT: A series of reactive (**2**, **4**) and nonreactive (**3**, **5**) fluorescent probes based on 4-(dimethylamino)-4'-nitrostilbene (**1**) have been synthesized. Substitution of a methyl on the dimethylamino group results in blue shifts in emission and increases in Φ_f , and corresponding reactive and nonreactive probes are indistinguishable. Emission spectra of **1**–**5** were recorded during the photoinitiated polymerization of methyl methacrylate (MMA). For nonreactive probes, only minor changes in emission are observed during the first 40% of the reaction, while at conversions between 50 and 90% λ_{\max} is proportional to the conversion. For reactive probes shifts of λ_{\max} during the early stages of the process are observed, enabling them to monitor the full polymerization process. It was proven that the shift in emission during the first stage of the reaction is due to covalent attachment of the reactive probes to the PMMA backbone.

Introduction

Fluorescent probes¹ have proven to be successful analytical tools for monitoring polymerization processes in real time² and for investigating various physical properties of polymers.³ Though information can be extracted from the probe's emission in different ways, e.g., by monitoring the emission intensity⁴ or the anisotropy of emission,⁵ monitoring the position of probe emission is the preferred method in many cases. No calibrations of individual samples are needed, geometrical constraints regarding the shape of objects do not apply, and standard fluorescent spectra without the use of additional optics can be used.⁶ Varieties of fluorescent probes have been developed in recent years for monitoring photoinitiated polymerization processes: excimer forming probes,⁷ twisted intramolecular charge transfer (TICT) probes,⁸ charge transfer (CT) probes,⁹ and organic salts.¹⁰ These probes exhibit pronounced blue shifts when a monomer is polymerized, but the mechanisms causing the blue shifts are fundamentally different.^{7–10}

Charge-transfer probes, which can be either of the D- π -A⁹ or D- σ -A¹¹ type, are the most sensitive. Previous research^{9a} has shown that the sensitivity of D- π -A probes for monitoring photoinitiated polymerization processes is roughly proportional to the sensitivity for solvent polarity (solvatochromism).^{11a,12} For 4-(dimethylamino)-4'-nitrostilbene (DMANS, **1**) blue shifts observed upon the polymerization of di(meth)acrylates readily exceed 100 nm. We chose **1** as the basis for the systematic development of novel fluorescent probes because it was both sensitive and easy to prepare. The incentive was to make a series of architecturally different probes, all containing a 4-(dialkylamino)-4'-nitrostilbene chromophore.^{13,14}

To this time, most experiments using fluorescent probes for monitoring photoinitiated polymerization processes have been carried out with nonreactive chro-

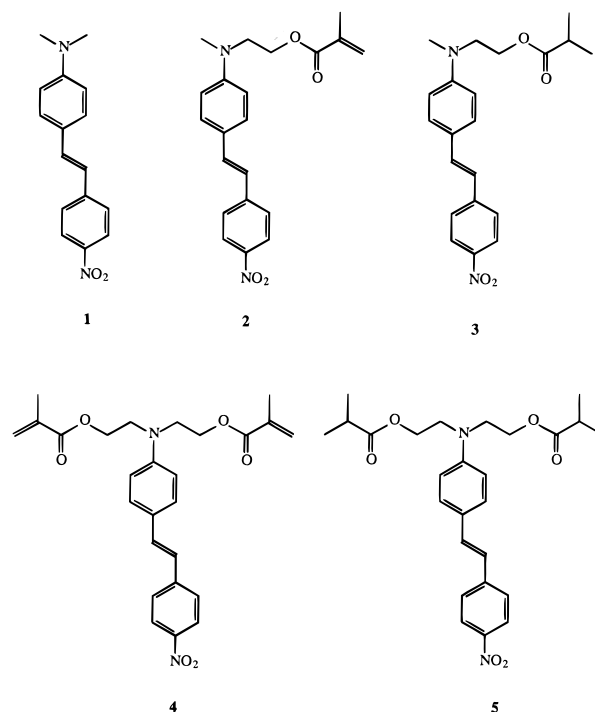


Figure 1. Fluorescent probes used in this research.

mophores such as **1**.^{15,16} From attaching a reactive group to the chromophore, fundamental changes can be expected in the interactions between a probe and the surrounding matrix. Nonreactive probes such as **1**, **3**, and **5** (Figure 1) dissolve in the unpolymerized monomer, as well as in the photoformed polymer, and are free to migrate within the constraints of the polymeric matrix. Whether the probe is evenly distributed or prefers to reside in specific areas, let alone which these areas are, is unknown. Reactive probes, like **2** and **4**, in which one or two methacrylate moieties are attached

to the chromophore, interact with their direct environment in a fundamentally different fashion. The probe dissolved in monomer will become covalently attached to the polymer backbone during the polymerization process, and significant differences in the emission of the reactive and the nonreactive probes are to be expected. It is also expected that, due to their immobilization during the polymerization process, reactive probes will be distributed evenly throughout the medium.¹⁷

Reactive probes **2** and **4**, as well as nonreactive probes **3** and **5** containing isobutyryl instead of methacryloyl esters, were synthesized. These probes allowed one to differentiate the effects of attaching a nonreactive spacer group to the chromophore and of covalently attaching the chromophore to the polymeric backbone. We also synthesized the polymers **P2** and **P4**, by copolymerization of the reactive probes **2** and **4** with 1000 equiv of MMA.¹⁸ These copolymers serve as model compounds for the polymers formed by incorporation of **2** and **4** during the photoinitiated polymerization of MMA.

The purpose of the work reported is to describe the synthesis and spectroscopic properties of the fluorescent probes **1–5**. The effects of small changes in molecular structure have been characterized spectroscopically in solvents of low viscosity of different polarities. Compounds **1–5** have been tested as fluorescent probes to monitor the photoinitiated polymerization of MMA so as to determine the effect of changing the molecular structure of the DMANS chromophore on its performance. In particular, the performance of reactive probes in comparison to nonreactive probes, i.e., determining the effect of attaching the probe to the polymer backbone, was investigated.

Experimental Section

General. Methyl methacrylate (MMA) was purchased from Merck-Schuchardt and was purified by distillation prior to use. Irgacure 907 (2-methyl-1-[4-(methylthio)phenyl]-2-morpholinopropanone-1) was a gift from Ciba-Geigy. 4-(Dimethylamino)-4'-nitrostilbene (**1**) was purchased from Kodak. Other reagents were purchased from Aldrich. Most solvents were reagent grade and used as provided. Dichloromethane and tetrahydrofuran were dried and purified by distillation from P₂O₅ and LiAlH₄, respectively. Triethylamine was dried by adding 4 Å molecular sieves.

Spectroscopic Measurements. Solvents for fluorescence and absorption spectra were spectrometric grade from Aldrich. Fluorescence measurements were recorded on a PTI Quanta-master spectrofluorimeter at right angles, using 420 nm as the excitation wavelength. Fluorescence quantum yields Φ_f were determined using samples that were degassed by ultrasound, employing 9,10-diphenylanthracene ($\Phi_f = 0.90$) as a reference.¹⁹ Solutions of PMMA in MMA were prepared by adding PMMA to solutions of fluorescent probe in MMA. Absorption spectra were recorded on a Contron Instruments UV-vis spectrometer. IR spectra were measured on a Mattson 6020 Galaxy Series FT-IR spectrometer. NMR spectra were recorded on a Varian XL 300 or 400 nuclear resonance spectrometer, using tetramethylsilane (TMS) as an internal standard.

Photoinitiated Polymerizations. Polymerization was achieved by exposing films to UV radiation from a 10W Philips PL10 low-pressure mercury lamp for successive periods of time. After each irradiation period films were analyzed by fluorescence or FT-IR spectroscopy. Irgacure 907 (1 wt %) was used as the photoinitiator, and 5×10^{-4} mol kg⁻¹ (typically 0.02 wt %) fluorescent probe was added. Films were made by squeezing a drop of monomer between NaCl plates divided by a 15 μ m Teflon spacer or microscope slides divided by 75 μ m

polypropylene spacers. A special metal holder embedded with rubber slabs to apply a high pressure without breaking the salt plates was used. Double-bond conversions were determined for films between NaCl plates by FT-IR spectroscopy. A correlation between the double-bond conversion of MMA and the emission maxima of **1** was obtained. All other measurements were made employing films between glass plates. GPC (gel-permeation chromatography) was performed on a Waters 410 apparatus with tetrahydrofuran as eluent. Polystyrenes with narrow molecular weight distributions were used as standards for calibration.

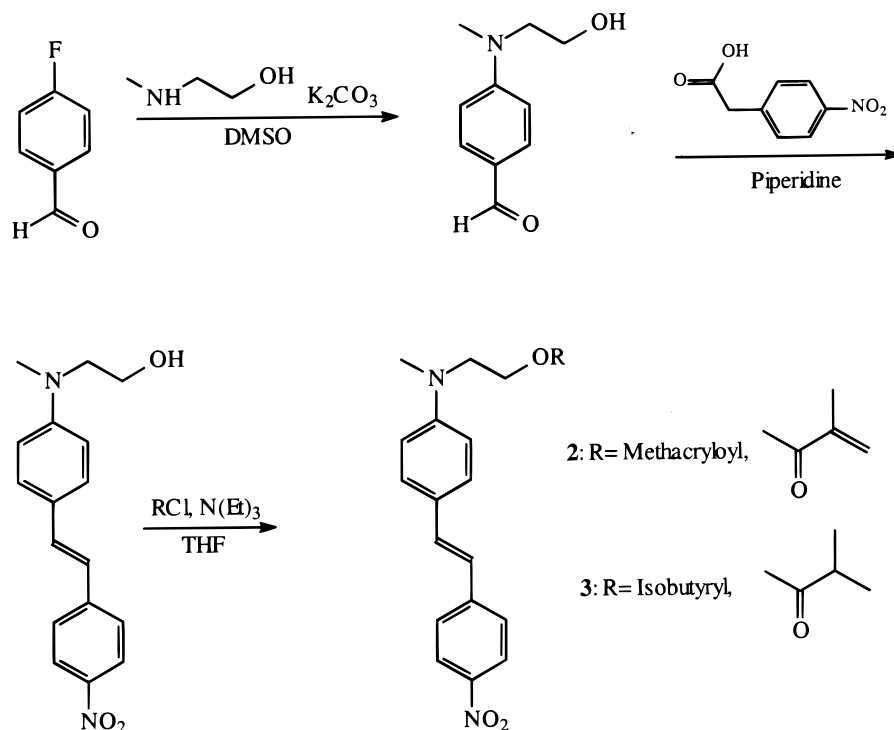
Synthesis. 4-[N-(2-Hydroxyethyl)-N-methylamino]-benzaldehyde, 7. Aldehyde **7** was synthesized according to the literature²⁰ and recrystallized from ethyl acetate; mp = 72 °C. ¹H NMR (CDCl₃, 400 MHz): 9.70 (s, 1H), 7.70 (d, *J* = 9.0 Hz, 2H), 6.75 (d, *J* = 9.0 Hz, 2H), 3.87 (t, *J* = 5.8 Hz, 2H), 3.62 (t, *J* = 5.8 Hz, 2H), 3.12 (s, 3H), 2.0 (br s, 1H). ¹³C NMR (CDCl₃, 100 MHz): 190.35, 153.91, 132.13, 125.42, 111.21, 60.10, 54.37, 39.19.

4-[N-(2-Hydroxyethyl)-N-methylamino]-4'-nitrostilbene, 8. 4.5 g (25.1 mmol) of **7** and 4.55 g (25.1 mmol) of 4-nitrophenylacetic acid were dissolved in 20 mL of piperidine and refluxed overnight. After evaporating the solvent, crude **8** was recrystallized in chlorobenzene, and a dark red crystalline solid was obtained. Yield 4.4 g (14.7 mmol = 59%) of **8**; mp = 185–187 °C. ¹H NMR (DMSO, 400 MHz): 8.17 (d, *J* = 8.8 Hz, 2H), 7.76 (d, *J* = 8.8 Hz, 2H), 7.49 (d, *J* = 8.8 Hz, 2H), 7.41 (d, *J* = 16.5 Hz, 1H), 7.10 (d, *J* = 16.5 Hz, 1H), 6.73 (d, *J* = 9.0 Hz, 2H), 4.71 (t, *J* = 5.1 Hz, 1H) 3.57 (m, *J* = 5.4 Hz, 2H), 3.45 (t, 2H), 2.99 (s, 3H).

4-[N-(2-Methacryloyloxyethyl)-N-methylamino]-4'-nitrostilbene, 2. To a solution of **8** (1.0 g, 3.35 mmol) in 100 mL of anhydrous dichloromethane at room temperature was added triethylamine (0.60 g, 5.9 mmol), and the solution was stirred for 15 min. The reaction mixture was cooled at 0 °C, and freshly distilled methacryloyl chloride (0.70 g, 6.7 mmol) in 10 mL of anhydrous dichloromethane was added. The resulting mixture was allowed to warm to room temperature and stirred overnight. After reaction the solution was extracted with water several times. The organic layer was dried over MgSO₄. The product, obtained after evaporating the solvent, was recrystallized from ethanol. Yield 0.95 g (2.59 mmol = 77%) of an orange crystalline solid; mp = 151–152 °C. ¹H NMR (CDCl₃, 400 MHz): 8.17 (d, *J* = 8.8 Hz, 2H), 7.55 (d, *J* = 9.0 Hz, 2H), 7.43 (d, *J* = 9.0 Hz, 2H), 7.19 (d, *J* = 16.2 Hz, 1H), 6.92 (d, *J* = 16.2 Hz, 1H), 6.74 (d, *J* = 9.0 Hz, 2H), 6.07 (s, 1H), 5.56 (s, 1H), 4.34 (t, *J* = 6.0 Hz, 2H), 3.70 (t, *J* = 6.0 Hz, 2H), 3.06 (s, 3H), 1.92 (s, 3H). ¹³C NMR (CDCl₃, 100 MHz): 167.33, 149.42, 145.96, 144.94, 136.08, 133.53, 128.53, 126.11, 125.97, 124.66, 124.16, 121.78, 112.08, 61.79, 50.86, 38.74, 18.31. Anal. Calcd for C₂₁H₂₂N₂O₄: C, 68.87; H, 6.00; N, 7.65. Found: C, 68.76; H, 5.98; N, 7.73.

4-[N-(2-Isobutyryloxyethyl)-N-methylamino]-4'-nitrostilbene, 3. To a solution of **8** (100 mg, 0.34 mmol) in 15 mL of anhydrous dichloromethane at room temperature was added triethylamine (70 mg, 0.69 mmol), and the solution was stirred for 15 min. The reaction mixture was cooled at 0 °C, and isobutyryl chloride (107 mg, 1.0 mmol, 3 equiv) in 2 mL of anhydrous dichloromethane was added. The resulting mixture was allowed to warm to room temperature and stirred overnight. The solution was extracted with water, and the organic layer was dried over MgSO₄. The product, obtained after evaporating the solvent, was recrystallized from ethanol. Yield 88 mg (0.24 mmol = 70%) of an orange crystalline solid; mp = 137–138 °C. ¹H NMR (CDCl₃, 300 MHz): 8.17 (d, *J* = 8.9 Hz, 2H), 7.55 (d, *J* = 8.9 Hz, 2H), 7.43 (d, *J* = 8.9 Hz, 2H), 7.19 (d, *J* = 16.2 Hz, 1H), 6.91 (d, *J* = 16.2 Hz, 1H), 6.73 (d, *J* = 8.9 Hz, 2H), 4.27 (t, *J* = 6.0 Hz, 2H), 3.65 (t, *J* = 6.0 Hz, 2H), 3.04 (s, 3H), 2.51 (sep, *J* = 7.0 Hz, 1H), 1.13 (d, *J* = 6.8 Hz, 3H). ¹³C NMR (CDCl₃, 75 MHz): 177.04, 149.45, 145.93, 144.95, 133.52, 128.52, 126.11, 124.60, 124.15, 121.73, 112.05, 61.35, 50.86, 38.70, 33.97, 18.31.

MS *m/z* 368 (M⁺), 267 (100%), 178, 43. Anal. Calcd for C₂₁H₂₄N₂O₄: C, 68.50; H, 6.52; N, 7.60. Found: C, 68.38; H, 6.50; N, 7.72.

Scheme 1. Synthesis of **2** and **3**

4-[N,N-Bis[2-(acetyloxy)ethyl]amino]benzaldehyde, 10. Aldehyde **10** was synthesized according to the literature.²¹ The compound was obtained as a thick oil that turns slightly blue and solidifies subsequently at room temperature. The crude product was used without further purification, despite small amounts ($\leq 5\%$) of 4-[N,N-bis[2-(acetyloxy)ethyl]amino]benzene.

4-[N,N-Bis[2-(hydroxyethyl)amino]-4'-nitrostilbene, 11. 7.5 g (2.69 mmol) of **10** and 4.0 g (2.21 mmol) of 4-nitrophenylacetic acid were dissolved in 20 mL of piperidine and refluxed overnight. After evaporating the solvent, crude **11** was recrystallized in chlorobenzene, yielding a dark red crystalline solid. Yield 4.0 g (1.22 mmol = 55%) of **11**; mp = 181–183 °C. ¹H NMR (DMSO, 400 MHz): 8.17 (d, $J = 9.0$ Hz, 2H), 7.75 (d, $J = 8.8$ Hz, 2H), 7.47 (d, $J = 9.0$ Hz, 2H), 7.40 (d, $J = 16.2$ Hz, 1H), 7.08 (d, $J = 16.6$ Hz, 1H), 6.73 (d, $J = 9.0$ Hz, 2H), 4.79 (t, $J = 5.3$ Hz, 2H), 3.57 (m, 4H), 3.47 (t, $J = 6.1$ Hz, 6H). ¹³C NMR (DMSO, 100 MHz): 148.59, 145.22, 144.99, 133.90, 128.59, 126.14, 123.95, 123.15, 120.54, 111.32, 58.06, 53.08.

4-[N,N-Bis[2-(methacryloyloxyethyl)amino]-4'-nitrostilbene, 4. To a solution of **11** (1.20 g, 36.5 mmol) in 100 mL of anhydrous dichloromethane at room temperature was added triethylamine (1.30 g, 128 mmol), and the solution was stirred for 15 min. The reaction mixture was cooled at 0 °C, and freshly distilled methacryloyl chloride (1.38 g, 132 mmol) in 10 mL of anhydrous dichloromethane was added. The resulting mixture was allowed to warm to room temperature and stirred overnight. The solution was extracted with water several times, and the organic layer was dried over MgSO₄. The product, obtained after evaporating the solvent, was recrystallized from ethanol, yielding an orange crystalline material; 1.44 g (31.2 mmol = 85%), mp = 76 °C. ¹H NMR (CDCl₃, 400 MHz): 8.18 (d, $J = 8.8$ Hz, 2H), 7.57 (d, $J = 8.8$ Hz, 2H), 7.44 (d, $J = 9.0$ Hz, 2H), 7.19 (d, $J = 16.5$ Hz, 1H), 6.93 (d, $J = 16.2$ Hz, 1H), 6.82 (d, $J = 9.0$ Hz, 2H), 6.20 (m, 2H), 5.68 (m, 2H), 4.35 (t, $J = 6.3$ Hz, 4H), 3.74 (t, $J = 6.3$ Hz, 4H), 1.95 (s, 6H). ¹³C NMR (DMSO, 100 MHz): 167.30, 147.90, 146.05, 144.82, 135.96, 133.27, 128.68, 126.19, 126.10, 125.18, 124.16, 122.17, 112.18, 61.62, 49.54, 18.33.

4-[N,N-Bis[2-(isobutyryloxyethyl)amino]-4'-nitrostilbene, 5. To a solution of **11** (200 mg, 0.61 mmol) in 30 mL of anhydrous dichloromethane at room temperature was added triethylamine (260 mg, 2.44 mmol), and the solution was

stirred for 15 min. The reaction mixture was cooled at 0 °C, and isobutyryl chloride (250 mg, 2.48 mmol) in 5 mL of anhydrous dichloromethane was added. The resulting mixture was allowed to warm to room temperature and stirred overnight. The solution was extracted with water and dried over MgSO₄. The product, obtained after evaporating the solvent, was purified by column chromatography on a SiO₂ column using ether as eluents. The thick deep red oil slowly crystallizes to form an orange solid; yield 220 mg (0.47 mmol = 77%), mp = 50 °C. ¹H NMR (CDCl₃, 400 MHz): 8.36 (d, $J = 9.0$ Hz, 2H), 7.80 (d, $J = 9.0$ Hz, 2H), 7.44 (d, $J = 8.9$ Hz, 2H), 7.38 (d, $J = 16.2$ Hz, 1H), 7.07 (d, $J = 16.3$ Hz, 1H), 6.79 (d, $J = 8.9$ Hz, 2H), 4.27 (t, $J = 6.3$ Hz, 4H), 3.67 (t, $J = 6.3$ Hz, 4H), 2.55 (sep, $J = 7.0$ Hz, 2H), 1.16 (d, $J = 6.9$ Hz, 12H). ¹³C NMR (DMSO, 100 MHz): 177.06, 147.91, 146.04, 144.82, 133.28, 128.66, 126.19, 125.11, 124.16, 122.13, 112.12, 61.16, 49.52, 33.94, 18.95.

Polymerization Procedure.¹⁸ Polymerizations were carried out by heating 1.0 g of a MMA/probe mixture (MMA/probe in a 1000:1 molar ratio) and 20 mg of α,α' -azobis(isobutyronitrile) (AIBN) in 10 g of dry benzene at 65 °C for 72 h. The reactions were performed in polymerization tubes, which were sealed under vacuum after several freeze–pump–thaw cycles. After precipitation in excess methanol and drying in vacuo 0.8 g of polymer was obtained.

P2, poly(MMA-co-2): $M_n = 36\,000$, $M_w = 71\,000$, Pd = 1.97, $\lambda_{em}(\text{MMA}) = 662$, $\Phi_f(\text{MMA}) = 0.11$.

P4, poly(MMA-co-4): $M_n = 30\,500$, $M_w = 52\,600$, Pd = 1.72, $\lambda_{em}(\text{MMA}) = 642$, $\Phi_f(\text{MMA}) = 0.17$.

Results and Discussion

Synthesis. The syntheses of **2**–**5** were performed according to Schemes 1 and 2.

The synthesis of **2** was previously described in the patent literature,²⁰ and compound **3** was synthesized in a similar fashion. The syntheses of **4** and **5** from **10**, a well-known compound,²¹ follow a similar route. Polymers **P2** and **P4** were obtained by a free radical polymerization of **2** and **4**, respectively, with 1000 equiv of MMA in benzene.

Spectroscopic Characterization. The emission spectra of **1**–**5** were recorded in a series solvents of low

Scheme 2. Synthesis of 4 and 5

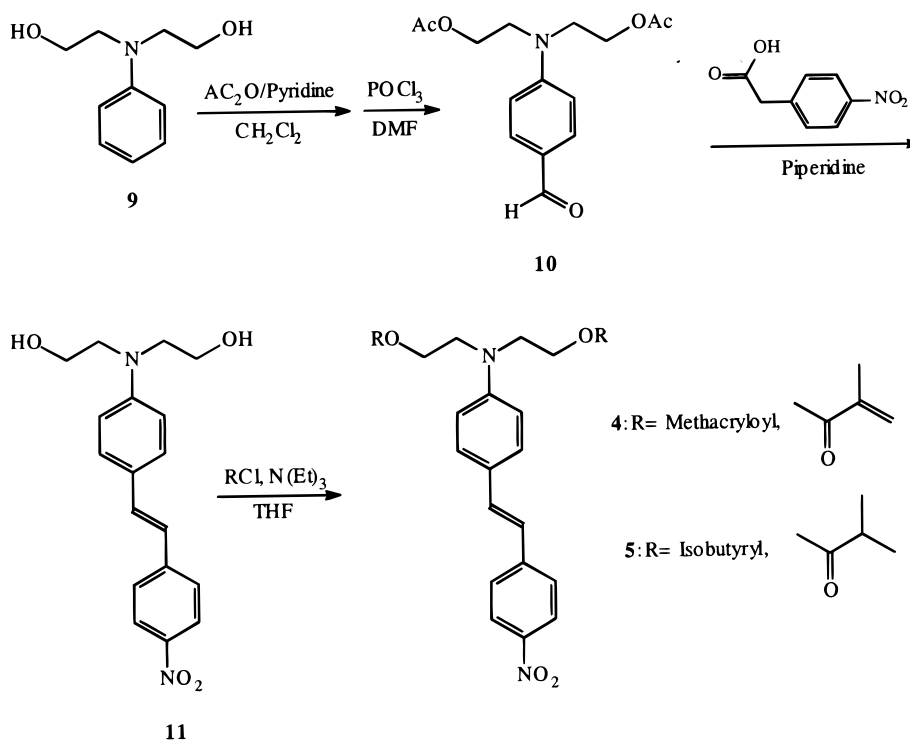


Table 1. Emission Maxima of 1–5 in Selected Solvents

solvent	Δf^{22}	λ_{\max} emission (nm)				
		1	2	3	4	5
cyclohexane	0.100	501 ^b	499 ^b	499 ^b	493 ^b	494 ^b
di- <i>n</i> -butyl ether	0.194	560	552	553	545	544
diisopropyl ether	0.237	582	573	573	544	563
diethyl ether	0.251	596	581	584	574	573
chloroform	0.251	725	709	710	696	696
MMA	0.275	684	669	668	656	655
ethyl acetate	0.292	684	671	670	658	657
tetrahydrofuran	0.308	683	668	668	653	654
1,2-dimethoxyethane	0.309	702	684	684	666	666
dichloromethane	0.319	758	734	735	716	718
acetone	0.375	767	746	747	728	727
acetonitrile	0.398	^a	798	798	776	776

^a No emission. ^b Vibrational structure in spectrum.

viscosity and different polarity.²² The data in Table 1 show that each of the probes are strongly solvatochromic in emission; large red shifts are observed upon increasing the polarity of the solvent.²³ Substitution of a methyl on the dimethylamino group with a 2-methacryloyloxyethyl or a 2-isobutyryloxyethyl group results in blue shifts of the emission. For **2** and **3** identical emission spectra are recorded, and shifts in λ_{\max} ranging from 2 nm in hexane to 24 nm in dichloromethane compared to **1** are observed. For **4** and **5** larger shifts compared to **1** are observed, ranging from 7 nm in hexane to 41 nm in dichloromethane. Clearly, blue shifts are of limited value in solvents of low polarity like hexane but increase as a function of the polarity of the solvent. Another effect of functionalizing the DMANS chromophore is the increase of emission intensity in polar solvents. Most striking is the observation that **2**–**5** are fluorescent in acetonitrile, a solvent in which no emission for **1** was detected.

The shape of the emission spectrum changes as a function of the solvent polarity for each of the probes. In cyclohexane the emission spectra exhibit vibrational structure, while perfect Gaussian emission spectra are

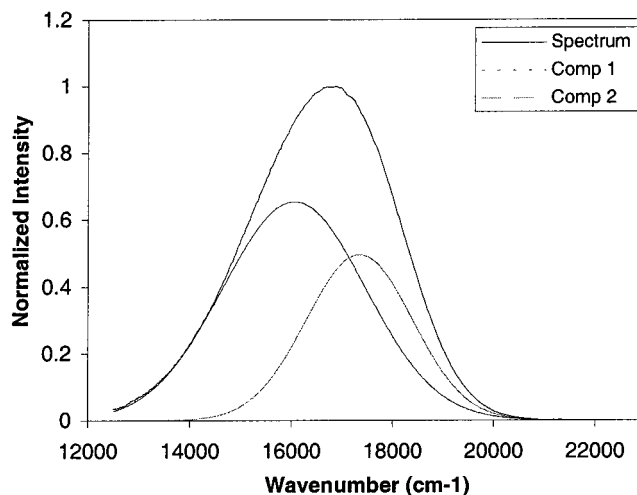


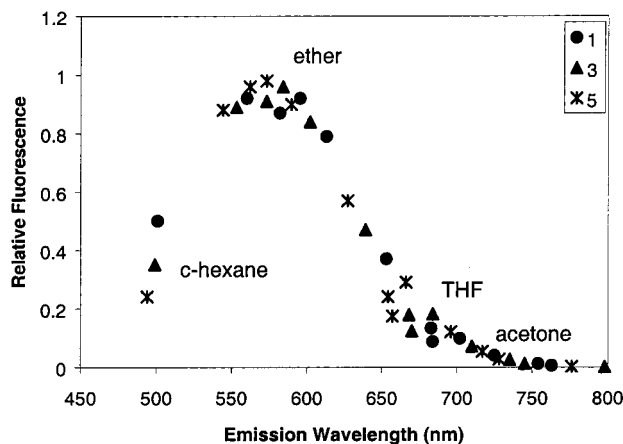
Figure 2. Emission spectrum of **1** in ether. The Gaussian distribution functions from which the spectrum is composed are also shown.

observed in solvents with a polarity exceeding that of ether. In solvents of intermediate polarity like dioxane, dibutyl ether, diisopropyl ether, and diethyl ether emission spectra cannot be described as simple Gaussian distribution functions. To a good approximation these spectra are described by two Gaussian components as illustrated in Figure 2. The long wavelength emission might result from a charge transfer (CT) state. The short wavelength emission most likely originates from a locally excited state.²⁴ In contrast to the emission from the locally excited state, the CT emission is quite sensitive to the polarity of the solvent (solvatochromism). Since an increase in solvent polarity lowers the energy of the CT state, exclusive formation of the CT state in polar solvents is anticipated.

The fluorescence quantum yields, Φ_f , of **1**–**5** in selected solvents (Table 2) show a sharp decrease in fluorescence quantum yield upon increasing the solvent

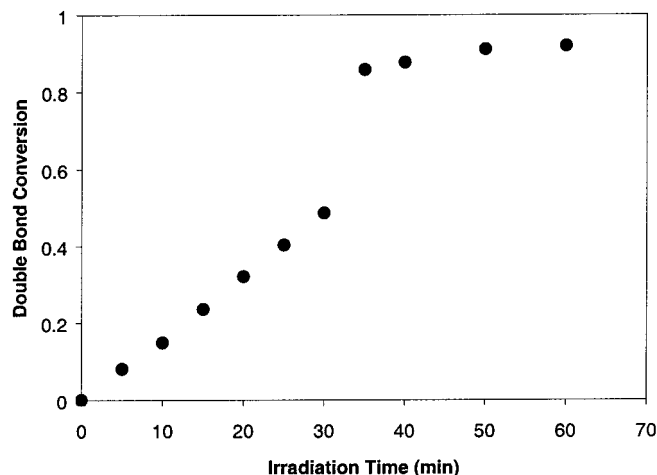
Table 2. Quantum Yields of the Fluorescent Probes 1–5 in Selected Solvents

solvent	Δf^{22}	Φ_f				
		1	2	3	4	5
cyclohexane	0.100	0.14	0.11	0.10	0.063	0.067
<i>n</i> -butyl ether	0.194	0.26	0.26	0.25	0.26	0.25
diisopropyl ether	0.237	0.24	0.26	0.26	0.27	0.27
diethyl ether	0.251	0.26	0.27	0.27	0.28	0.27
chloroform	0.251	0.011	0.02	0.02	0.034	0.34
mma	0.275	0.064	0.10	0.10	0.15	0.15
ethyl acetate	0.292	0.024	0.035	0.035	0.048	0.049
tetrahydrofuran	0.308	0.037	0.050	0.050	0.074	0.074
1,2-dimethoxyethane	0.309	0.027	0.051	0.051	0.066	0.067
dichloromethane	0.319	0.0032	0.0077	0.0073	0.016	0.015
acetone	0.375	2×10^{-4}	0.003	0.003	0.008	0.008
acetonitrile	0.398		3×10^{-4}	3×10^{-4}	6×10^{-4}	6×10^{-4}

Figure 3. Relative fluorescence quantum yields of 1, 3, and 5 as a function of the emission wavelength λ_{\max} .

polarity above that of ether for each of the probes. Attaching spacers to the DMANS chromophore (2–5) results in considerable increases of Φ_f in solvents with polarities above that of ether. In all cases the increase in Φ_f due to the attachment of spacers is accompanied by a blue shift in the emission maximum. As noted earlier, the emission wavelength λ_{\max} and the emission intensity I_{\max} of 1 are strongly correlated. Changes in the environment, either a decrease of polarity or a decrease in the mobility of “solvent” molecules, lead to blue shifts of λ_{\max} and increases of I_{\max} . By plotting Φ_f as a function of λ_{\max} for 1, 3, and 5 (Figure 3),²⁵ it is shown that each probe exhibits identical emission characteristics, since all the data points are positioned on one curve. The highest Φ_f values are found when probes emit between 610 and 560 nm a regime in which dual emission is found. Viewed from this perspective, the strong fluorescence in these solvents can be ascribed to the intense emission of both emitting states. In more polar solvents only one emitting species is present, the CT state, and Φ_f of this emission strongly decreases as the polarity of the solvent increases. This is a phenomenon commonly observed for CT emissions.

Photoinitiated Polymerization Processes. Formulations containing fluorescent probe and radical initiator were squeezed between glass plates divided by 75 μm polypropylene spacers, and emission spectra were recorded after subsequent irradiation periods of 5 min. In our experiments, the addition of a fluorescent probe effects the polymerization process. Competitive absorption by the fluorescent probes reduces the *initial* rate of polymerization of MMA by an estimated 30%. In addition, radicals generated by the photodecomposition of the photoinitiator bleach the probe molecules, thus

Figure 4. Double-bond conversion of MMA as a function of the irradiation time for 75 μm films between glass plates.

retarding the polymerization process slightly. One does not expect significant differences in reaction rate between formulations containing different probes, since equal amounts of probe are added to the solutions and their absorption spectra are similar. When corresponding reactive and nonreactive probes are employed, differences in reaction rates can be excluded.

Double-bond conversions of MMA as a function of the irradiation time, measured for formulations containing 1 as the fluorescent probe (Figure 4), resemble those reported for the thermal polymerizations of MMA.²⁶ The reaction rate is low up to a conversion of 50%. Subsequently, the reaction rate increases dramatically, due to the so-called autoacceleration effect,²⁷ and the conversion increases to 85%. After reaching this degree of conversion, the rate of polymerization strongly decreases due to vitrification of the matrix, and after 60 min of irradiation, the reaction virtually stops at a 92% conversion. Quantitative double-bond conversions can be obtained from leaving the sealed samples in the dark (60 + ac in Table 3).

The polymers formed photochemically were isolated by precipitation from methanol. When reactive probes 2 and 4 were employed, slightly yellow, fluorescent polymers were isolated from colorless methanol. Emissions wavelengths of these polymers in MMA, 661 and 642 nm, respectively, are identical to those recorded for P2 and P4. In contrast, white and nonfluorescent polymers were isolated in all the other cases. The methanol phase was slightly yellow when nonreactive probes were employed, indicating the presence of the dialkylamino chromophore in the solution. These experiments prove that covalent incorporation of reactive

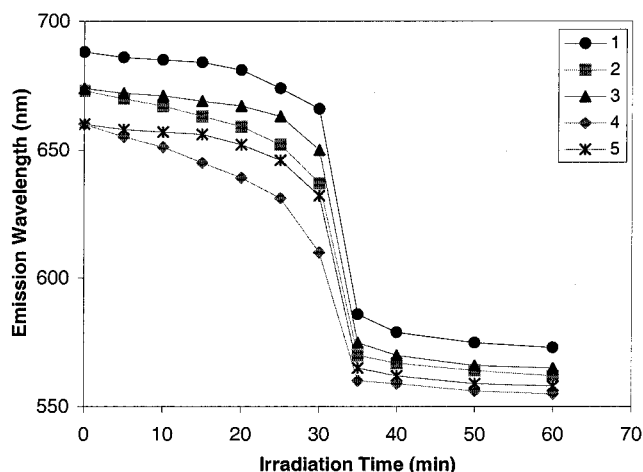


Figure 5. Emission wavelength λ_{\max} of 1–5 in MMA as a function of the irradiation time.

Table 3. Fluorescence Maxima of 1–5 in MMA as a Function of the Irradiation Time

irradiation time (min)	λ_{\max} (nm)				
	1	2	3	4	5
0	688	673	674	660	660
5	686	670	672	655	658
10	685	668	670	651	657
15	684	663	669	645	656
20	681	659	667	639	652
25	674	652	663	631	646
30	666	637	650	610	632
35	586	570	575	560	565
40	579	567	570	559	562
50	575	564	566	556	559
60	573	562	565	555	558
60 + ac	556	552	555	542	546

probes into the polymer that is formed has occurred and also suggest that the incorporation is efficient.²⁸ GPC chromatograms for the polymers were identical regardless of the probe.²⁹

Emission Spectra. (a) Emission Wavelength. The emission wavelengths (λ_{\max}) found for 1–5 during the photoinitiated polymerization of MMA are shown in Table 3 and Figure 5. In MMA these are completely in line with their emissions in solvents of low viscosity. Attachment of one spacer (2 and 3) leads to a 15 nm blue shift, while attachment of two spacers (4 and 5) leads to a 30 nm shift in emission.

One can clearly distinguish the various stages of the polymerization of MMA; the reaction before, autoacceleration between 30 and 35 min of irradiation, and the subsequent slow reaction in a polymer glass by monitoring the emission spectra of all probes as a function of the irradiation time. In initial stages of the reaction reactive probes 2 and 4 respond in a different fashion from nonreactive probes 1, 3, and 5. While the emission wavelengths λ_{\max} of 1, 3, and 5 shift marginally, a gradual blue shift of λ_{\max} of the reactive probes 2 and 4 is observed. In a control experiment 1–5 are dissolved in MMA and increasing concentrations of PMMA added. Addition up to 40% of PMMA results in limited blue shifts comparable to those reported for the nonreactive probes during the photoinitiated polymerization reaction. The emission spectra of the corresponding reactive (2, 4) and nonreactive probes (3, 5) were not distinguishable, since each of the probes is dissolved in a homogeneous PMMA solution.

The emission spectra of all probes are strongly blue-shifted between 30 and 35 min of irradiation, indicating

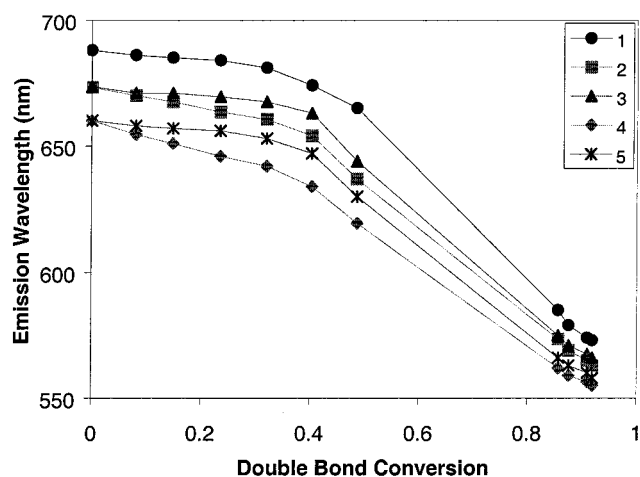


Figure 6. Emission wavelength λ_{\max} of 1–5 in MMA as a function of the double-bond conversion for photoinitiated polymerization reactions.

profound changes in the medium surrounding the probes. Subsequently and as the polymerization process slowly proceeds, small blue shifts in the emission of 1–5 are observed. In the final product obtained after a 60 min irradiation period, λ_{\max} values of the probes are found not to be identical. Compared to 1, probes 2 and 3 are blue-shifted 10 nm, while 4 and 5 are blue-shifted 15 nm. The final wavelengths of emission of the reactive probes 2 and 4 are slightly blue-shifted (~3 nm) when compared to their nonreactive counterparts 3 and 5. When the double-bond conversion increases from 92 to 100% upon standing this leads to further blue shifts (typically 10–15 nm) in the emission spectra of all probes. Though one cannot exclude other effects such as conformational changes in the polymer matrix, especially in cases where samples were heated to accelerate the postcure, these blue shifts indicate the probes to be extremely sensitive to double-bond conversion even at these high conversions.

The λ_{\max} values found for 1–5 are plotted as a function of the double-bond conversion in Figure 6. Major differences are observed between these probes in polymer solution before autoacceleration occurs. Non-reactive probes exhibit the typical behavior that was previously reported for 1. Before autoacceleration in a polymer solution with a PMMA content of up to 40%, the λ_{\max} is hardly effected by the presence of PMMA, while at higher conversions λ_{\max} strongly decreases with increasing conversion. For reactive probes 2 and 4, a clear correlation between λ_{\max} and double-bond conversion is observed to occur even at low conversions. The observed spectra are composed of that of the free probe (2 or 4) and a polymeric probe (P2 or P4). Emission spectra of these species in MMA have been recorded, and the blue shift of the polymeric probes P2 and P4 compared to 2 and 4 are 7 and 14 nm, respectively. In addition, the polymeric probes have a 10% higher fluorescence quantum yield. It might be that these differences increase during the polymerization process, but this has not been investigated. Incorporation of reactive probes can be demonstrated by comparing the emission wavelengths of the reactive and nonreactive probes obtained during polymerization reactions with those obtained from PMMA/MMA solutions. Figure 7 demonstrates that for the reactive probe 4 the λ_{\max} values obtained during the polymerization are significantly lower than are those in PMMA/MMA mixtures.

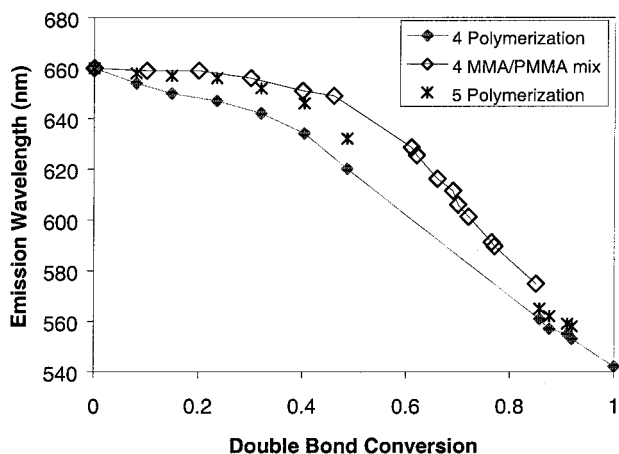


Figure 7. Emission wavelength λ_{\max} of **4** and **5** during a photoinitiated polymerization reactions and λ_{\max} of **4** in PMMA/MMA mixtures as a function of the double-bond conversion.

For the nonreactive probe **5**, on the other hand, the corresponding λ_{\max} values are virtually identical in most of the data points.

After autoacceleration the behaviors of the reactive and the nonreactive probes are similar. A linear relationship between λ_{\max} and double-bond conversion is expected for both the reactive and the nonreactive probes. This relationship cannot be obtained from polymerization experiments directly due to a lack of data points. However, such a relationship can be obtained for the nonreactive probes by recording emission spectra in independently prepared PMMA/MMA mixtures. We anticipate a similar relationship between λ_{\max} and the double-bond conversion when reactive probes are employed, since the effects of covalent attachment are rather subtle compared to the shifts in λ_{\max} at this stage of the reaction.

(b) Emission Intensity One can follow the polymerization process by monitoring the intensity of the emission of the fluorescent probes (I_{\max}). Measuring intensity of emission from thin films is not as accurate as measuring the emission wavelength, since the intensity measured is sensitive to the exact position of the film and reflections at different interfaces leading to errors on the order of 5–10%. Also photobleaching, a process resulting in probe decomposition, takes place during the course of the polymerization process. The extent of photobleaching is extreme in MMA; 70% of the probe molecules become bleached, not by direct irradiation, but from attack of the photoformed radicals on the probe. The extent of bleaching was found to be similar for **1–5**, though subtle differences cannot be excluded.

Typical emission intensities obtained from **1–5** during photoinitiated polymerizations of MMA are depicted in Figure 8. Initially all probes evidence a decrease in I_{\max} . Employing **1** as a fluorescent probe, it was demonstrated that a slight increase in fluorescence quantum yield Φ_f occurs at these conversions but that a strong decrease in the number of probe molecules due to photobleaching causes the observed decrease in I_{\max} . A sharp increase in emission intensity during autoacceleration is observed for all the probes. As the medium changes from a viscous polymer solution to a glassy polymer film, the fluorescence quantum yield Φ_f is strongly increased. Subsequently as the polymerization proceeds slowly, the emission intensity decreases once more, but not as pronounced as during the first 20 min of the process.

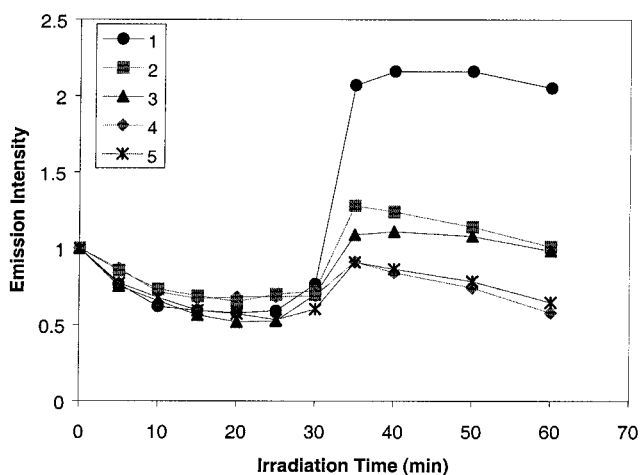


Figure 8. Emission intensity I_{\max} of **1–5** in MMA as a function of the irradiation time.

In this stage of the reaction photobleaching is strongly retarded, but the increase in Φ_f is slower.

Differences in performances of the probes are clearly visible. For **1**, the increase of I_{\max} after the polymerization is completed exceeds that of **2** and **3**, which, in turn, is larger than that for **4** and **5**. The lessened gain in magnitude of the emission intensity as the chromophore is functionalized follows directly from the quantum yields of emission Φ_f for the probes in MMA: $\Phi_f(\mathbf{1}) < \Phi_f(\mathbf{2/3}) < \Phi_f(\mathbf{4/5})$, Table 3. Since it is expected that Φ_f in PMMA films is similar for all the probes, the largest increase in Φ_f should be observed for **1**. Another striking observation is that during the first stages of the polymerization, up to 30 min irradiation, the decrease in I_{\max} is markedly slower for the reactive probes **2** and **4**. A higher intensity of emission for the reactive versus the corresponding nonreactive probes before autoacceleration can be explained by covalent attachment of the probe to the backbone. On the basis of a 10% higher Φ_f for **P2** and **P4** compared to that for **2** and **4**, the emission intensity of the reactive probes is expected to be up to 5% higher before autoacceleration occurs. In addition, a stronger increase in Φ_f and a slightly lower photobleaching for **P2** and **P4** compared to those for **2** and **4** is expected.

(c) Half-Width and Shape. The half-width of an emission can be indicative of the homogeneity of the environment in which a probe is incorporated. If the probe is present in differing environments, different emitting species will be present, and the resulting emission spectrum will be broader than any of the contributing spectra. Also, the shape of the emission spectrum can be distorted. The emission spectra of **1–5** during the polymerization of MMA were analyzed, and results are presented; see Figure 9.

Attachment of substituents to the amino group increases the half-widths of the probes in MMA by 100 cm^{-1} per substituent. Incorporating the probe in the polymer backbone results in even higher half-widths; the half-width of **P2** is 400 cm^{-1} above that of **1** in MMA. A broadening of the emission spectra of each of the probes is observed during the polymerization before autoacceleration. The increase in the half-width of the reactive probes is roughly twice that of their nonreactive counterparts. This is not surprising since the emission spectra of the reactive probes are composed of the emission spectra of free and attached probe, and these are two spectroscopically different species. In addition,

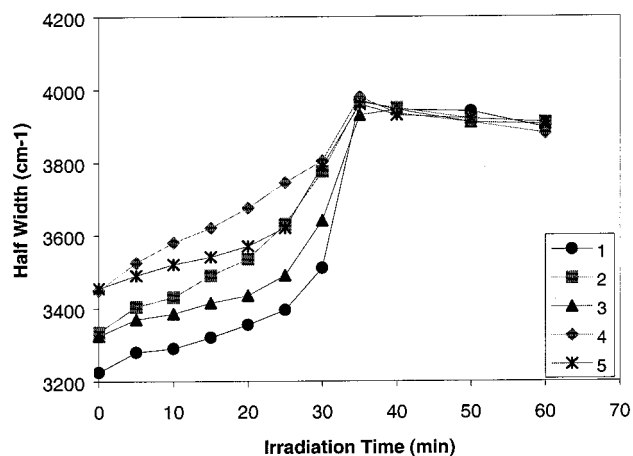


Figure 9. Peak width of 1–5 in MMA (in cm^{-1}) as a function of the irradiation time.

the half-widths of polymer bound probes **P2** and **P4** are nearly 300 cm^{-1} larger than are those of **2** and **4**. Control experiments, in which the half-widths of 1–5 in MMA/PMMA mixtures were determined, revealed monotonic increases of the half-widths upon increasing [PMMA] comparable to those observed for **1**, **3**, and **5** in the photopolymerization process. Sharp increases in half-widths are observed between 30 and 35 min after the irradiation is begun, particularly in the case of the nonreactive probes. After autoacceleration, as a polymer glass is formed, the half-widths of each of the probes are identical within experimental error. During the latter stages of the reaction, small decreases in half-widths are observed for all probes.

We have analyzed the shape of the emissions of 1–5 during the polymerization reaction. Up to 30 min irradiation, spectra of all probes are described by a single Gaussian distribution function (Figure 10). This does not imply that only one emitting species is present, since it is known that when the reactive probes are employed two emitting species are present: the reactive probes **2** or **4** and polymer bound probes **P2** or **P4**. These species have Gaussian emission spectra that are only 10–20 nm apart, and the resulting spectra are still described by single Gaussian distribution functions. After 35 min of irradiation, the emission spectra are no longer described by a single Gaussian distribution function. Instead, the emission spectra of 1–5 in a glassy polymer are described accurately as being composed of a broad long wavelength emission and a narrow emission at shorter wavelength. This is illustrated by Figure 10b,c, which displays the emission spectra of **4** at different stages, along with the components comprising these emissions. As polymerization commences, the relative amount of the short wavelength component steadily increases. Significant differences between the emission spectra of the reactive and nonreactive probes are not observed. Clearly the differences in emission spectra between the free probe molecules and the polymer bound probes are too small to induce dual emission.

Dual emission indicates that the probe emits either from two different excited states or from one excited state in two distinctly different environments. For probes 1–5 dual emission is generally observed as the emission wavelength λ_{max} drops below 630 nm. This dual emission is observed in all kinds of media including solvents of low polarity. Clearly the dual emission observed here does not necessarily indicate that the

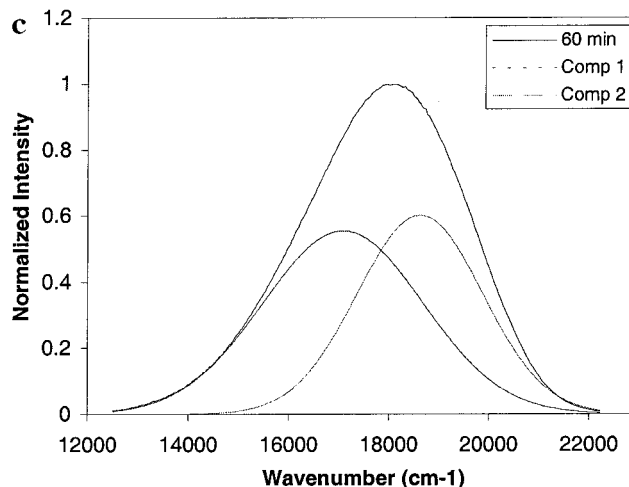
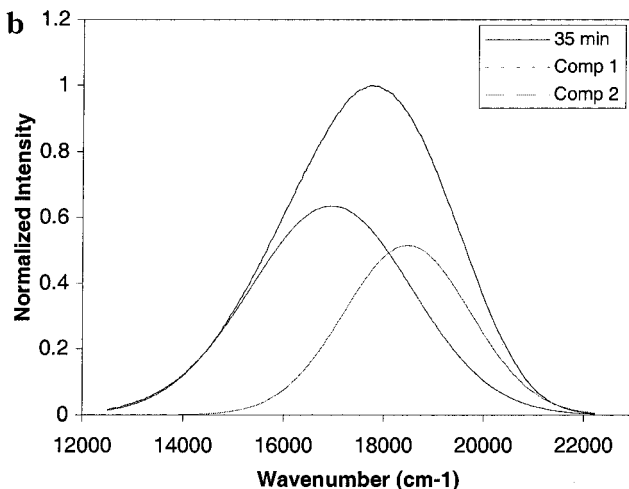
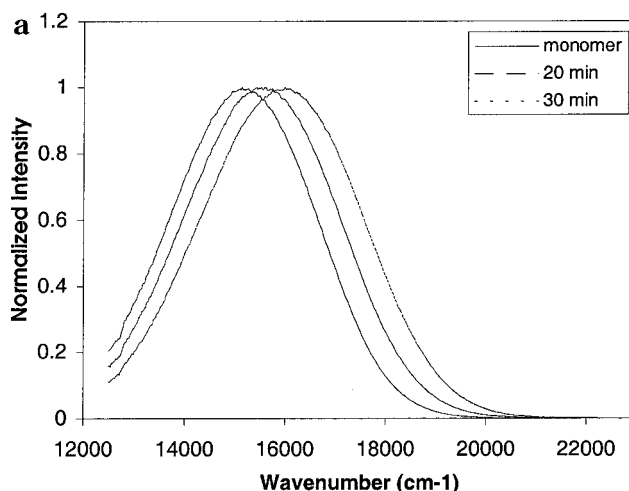


Figure 10. Emission spectra of **4** in MMA after irradiation periods of (a) 0–30 min, (b) 35 min, and (c) 60 min.

probe in the polymer formed photochemically is emitting from two distinct phases in a heterogeneous environment.

Conclusions

We have synthesized and characterized a series of derivatives of 4-(dimethylamino)-4'-nitrostilbene (DMANS, **1**), **2**–**5**, and employed them as fluorescent probes for monitoring the photoinitiated polymerization of MMA. Replacing one or two methyl groups of the DMANS chromophore by a 2-methacryloyloxyethyl or

a 2-isobutyryloxyethyl group yields fluorescent molecules with a slightly modified spectroscopic behavior. In every case molecules containing methacryloyl esters or isobutyryl esters are spectroscopically indistinguishable. The effects of substitution are additive and result in minor blue shifts in absorption and considerable blue shifts in emission. The blue shifts in emission increase as the polarity of the solvent increases and may reach values of 20 nm per substitution. Also, these blue shifts are accompanied by increases in the fluorescence quantum yield Φ_f .

DMANS derivatives **1**–**5** are sensitive fluorescent probes suitable for monitoring the photoinitiated polymerization of MMA. Stages of the reaction, before, during, and after autoacceleration can be clearly distinguished, especially when nonreactive probes are employed. The nonreactive probes **1**, **3**, and **5** do not monitor the polymerization of MMA before autoacceleration, since only minor changes in their emission maxima are found. The reactive probes **2** and **4** monitor the polymerization process before autoacceleration, due to covalent attachment to the polymer backbone. Significant blue shifts of λ_{\max} are observed along with considerable increases of the half-widths. Dimethacrylate **4** is more sensitive than the methacrylate **2** due to incorporation of two methacrylates in the polymer backbone.

On the basis of the sensitivity of reactive probes during the first stages of the MMA polymerization, we conclude that reactive fluorescent probes are useful in a wider range of applications than nonreactive probes. Reactive probes are incorporated in the polymer chain, thereby forming a different emitting species. Providing that these species emit at different wavelengths, reactive probes monitor these polymerization processes directly. Notably for monitoring polymerization processes in which the polymer–monomer mixture forms a homogeneous solution, only reactive probes are sensitive throughout the reaction. Research in this area is currently being undertaken.

Acknowledgment. This research was funded by the Royal Netherlands Academy for Arts and Sciences (KNAW). Part of this work has been supported by the Office of Naval Research (ONR-N00014-91-J-1921) and the Natural Science Foundation (DMR 90-13109). The authors thank Drs. J. M. Warman and R. D. Abellon (IRI, Delft University of Technology) for helpful discussions and the use of experimental facilities.

References and Notes

- (1) (a) For a review on fluorescent sensors and switches, see: de Silva, A. P.; Nimal Gunaratne, H. Q.; Gunnlaugsson, T.; Huxley, A. J. M.; McCoy, C. P.; Rademacher, J. T.; Rice, T. E. *Chem. Rev.* **1997**, *97*, 1515. (b) For a review on fluorescent probes for monitoring photoinitiated polymerization processes, see: Neckers, D. C.; Jager, W. F. *Chemistry & Technology of UB & EB Formulations for Coatings, Inks and Paints*, John Wiley and Sons: New York, 1998; Vol. 7, Chapter 3.
- (2) (a) Hu, S.; Polpielar, R.; Neckers, D. C. *Macromolecules* **1998**, *31*, 4107. (b) Polpielar, R.; Neckers, D. C. *RadTech Proc.* **1996**, *1*, 271. (c) Paczkowski, J.; Neckers, D. C. *Macromolecules* **1992**, *25*, 548.
- (3) (a) Morawetz, H. J. *Polym. Sci., Polym. Chem. Ed.* **1999**, *37*, 1725. (b) Miller, K. E.; Krüger, R. H.; Torkelson, J. M. *J. Polym. Sci., Polym. Phys. Ed.* **1995**, *22*, 2343. (c) Shea, K. J.; Stoddard, G. J.; Sasaki, D. Y. *Macromolecules* **1989**, *22*, 4303. (d) Shea, K. J.; Sasaki, D. Y.; Stoddard, G. J. *Macromolecules* **1989**, *22*, 1722. (e) Loutfy, R. O.; Teergarden, D. M. *Macromolecules* **1983**, *16*, 452.
- (4) (a) Loutfy, R. O. *Macromolecules* **1981**, *14*, 270. (b) Loutfy, R. O. *J. Polym. Sci., Polym. Phys. Ed.* **1982**, *20*, 825.
- (5) For an example see: van Ramensdonk, H. J.; Vos, M.; Verhoeven, J. W.; Möhlmann, G. R.; Tissink, N. A.; Meesen, A. *Polymer* **1987**, *28*, 951.
- (6) In our research group we have developed a fiber optics based fluorimeter that uses a CCD recorder that can take emission spectra in as little as 25 ms; see refs 2a and 2b.
- (7) (a) Valdez-Aguilera, O.; Pathak, C. P.; Neckers, D. C. *Macromolecules* **1990**, *23*, 689. (b) Wang, F. W.; Lowry, R. E.; Grant, W. H. *Polymer* **1984**, *25*, 690.
- (8) (a) Paczkowski, J.; Neckers, D. C. *Macromolecules* **1991**, *24*, 3013. (b) Rettig, W. *Angew. Chem., Int. Ed. Engl.* **1986**, *25*, 971.
- (9) (a) Jager, W. F.; Volkers, A. A.; Neckers, D. C. *Macromolecules* **1995**, *28*, 8, 8153. (b) Jager, W. F.; Lungu, A.; Chen, D. Y.; Neckers, D. C. *Macromolecules* **1997**, *30*, 780. (c) Schaecken, Warman, J. M. *J. Phys. Chem.* **1995**, *99*, 6145.
- (10) Jager, W. F.; Kudasheva, D.; Neckers, D. C. *Macromolecules* **1996**, *29*, 7351.
- (11) (a) Mes, G. F.; de Jong, B.; van Ramensdonk, H. J.; Verhoeven, J. W.; Warman, J. M.; de Haas, M. P.; Horsman van den Dool, L. E. W. *J. Am. Chem. Soc.* **1984**, *106*, 6524. (b) Hermant, R. M.; Bakker, N. A. C.; Scherer, T.; Krijnen, B.; Verhoeven, J. W. *J. Am. Chem. Soc.* **1990**, *112*, 1214. (c) For the use of D-σ-A probes in polymers, see: Verheij, H. J. *Fluorescence Probing of Polymers*. Ph.D. Thesis, University of Amsterdam, 1997.
- (12) (a) Reichardt, C. *Chem. Rev.* **1994**, *94*, 2319. (b) Lippert, E. *Z. Electrochem.* **1957**, *61*, 962.
- (13) For the use of DMANS as a solvatochromic probe in microheterogeneous media, see: Shin, D. M.; Whitten, D. G. *J. Phys. Chem.* **1988**, *92*, 2944.
- (14) For the fluorescence of DMANS in various solvents, see: (a) Gruen, H.; Görner, H. *J. Phys. Chem.* **1989**, *93*, 7144. (b) Lippert, E.; Lüder, W.; Moll, F.; Nägele, W.; Boos, H.; Prigge, H.; Seibold-Blankenstein. *Angew. Chem.* **1961**, *73*, 695.
- (15) For the emission of reactive fluorescent probes and fluorescent reactants during thermal polymerizations, see: (a) Phelan, J. C.; Sung, C. S. P. *Macromolecules* **1997**, *30*, 6845. (b) Huang, X. Y.; Yu, W.; Sung, C. S. P. *Macromolecules* **1990**, *23*, 390. (c) Sung, C. S. P.; Mathisen, R. *Polymer* **1987**, *28*, 941.
- (16) Recently the incorporation of a maleimido functionalized probe during the polymerization of MMA by γ-irradiation was reported. See: Warman, J. M.; Abellon, R. D.; Verheij, H. J.; Verhoeven, J. W.; Hofstra, J. W. *J. Phys. Chem. B.* **1997**, *101*, 4913.
- (17) Extrusion of probe molecules may lead to enrichment of nonreactive probes in those regions that polymerize later in the process.
- (18) Polymer bound fluorescent probes such as **P2** and **P4** will be discussed in a subsequent paper.
- (19) Eaton, D. F. *Pure Appl. Chem.* **1988**, *7*, 1107.
- (20) The synthesis of **2** is reported in: Garo, K.; Donald, R.; Alan, B.; Calundann, G. W.; East, A. J. U.S. Patent 4,957,655, Sept 18, 1990, submitted to Hoechst Celanese.
- (21) Moon, K.-J.; Shim, H.-K.; Lee, K.-S.; Zieba, J.; Prasad, P. N. *Macromolecules* **1996**, *29*, 861.
- (22) Absorption spectra of **1**–**5** were almost identical. Small blue shifts, typically 2 nm for each substituent, were observed.
- (23) The solvent parameter Δf is defined as: $\Delta f = (\epsilon - 1)/(2\epsilon + 1) - (n^2 - 1)/(4n^2 + 2)$ in which ϵ is the dielectric constant and n is the optical refractive index of the solvent; see ref 11a.
- (24) The occurrence of dual emission from an ICT state and a non-CT state closely resembles the photophysics described for TICT probes; see ref 8b.
- (25) In all solvents $\Phi_2 = \Phi_3$ and $\Phi_4 = \Phi_5$.
- (26) (a) Balke, S. T.; Hamielec, A. E. *J. Appl. Polym. Sci.* **1973**, *17*, 905. (b) Trommsdorff, E.; Köhle, H.; Lagally, P. *Makromol. Chem.* **1948**, *1*, 169. (c) Norrish, R. G. W.; Brookman, E. F. *Proc. R. Soc. London, Ser. A* **1939**, *171*, 147.
- (27) O'Neil, G. A.; Torkelson, J. M. *Trends Polym. Sci.* **1997**, *5*, 349.
- (28) A series of polymers with chromophore contents up to 10% were obtained by copolymerization of **2** with MMA in benzene solution (experimental). A higher degree of functionalization did not decrease the molecular weight of the polymer significantly. This proves that incorporation of **2** does not terminate the polymerization and suggests an even distribution of **2** in the polymer.
- (29) GPC chromatograms have a bimodal shape with maxima at 50 000 and 160 000, similar to those reported for thermal polymerizations of MMA; see ref 26a.